Acta Crystallographica Section D
Biological Crystallography
ISSN 0907-4449

Ligand-binding and metal-exchange crystallographic studies on shrimp alkaline phosphatase

Maaike M. E. de Backer,[a] Sean McSweeney,[a] Peter F. Lindley[a,b] and Edward Hough[c]*

[a]European Synchrotron Radiation Facility, France, [b]Instituto de Tecnologia Quimica e Biologica, Portugal, and [c]University of Tromsø, Norway

Correspondence e-mail: edward.hough@chem.uit.no

Received 28 October 2003
Accepted 25 June 2004

PDB References: SAP–PNPP complex, 1shn, r1shnsf; SAP–Mg complex, 1shq, r1shqsf.

Alkaline phosphatases (APs) are homodimeric metalloenzymes that catalyze the hydrolysis and transphosphorylation of phosphate monoesters. Each monomer contains a metal-binding triad that for optimal activity is usually occupied by two zinc ions and one magnesium ion. The recently determined crystal structure of cold-active shrimp alkaline phosphatase (SAP) was, however, fully occupied by zinc ions. This paper describes a metal-exchange experiment in which the zinc ion in one binding site (referred to as the M3 site) is replaced by magnesium. Crystal structures revealed a concomitant structural change: the metal exchange causes movement of a ligating histidine into a conformation in which it does not coordinate to the metal ion. The M3 site is relevant to catalysis: its occupation by magnesium is postulated to favour catalysis and it has been suggested to be a regulatory site for other APs. Further crystallographic studies show that ligand binding can induce a conformational change of an active-site arginine from a 'non-docked' (non-interacting) to a 'docked' conformation (interacting with the ligand). The first conformation has only been observed in SAP, while the latter is common in available AP structures. The observation that the arginine does not always bind the substrate may explain the increased catalytic efficiency that is generally observed for cold-active enzymes.

1. Introduction

In biological systems, hydrolysis of phosphate monoesters is an important process linked to energy metabolism, metabolic regulation and a variety of cellular signal-transduction pathways (Vincent *et al.*, 1992). Alkaline phosphatases (APs; EC 3.1.3.1) are homodimeric metalloenzymes that catalyze the hydrolysis or, in the presence of phosphate acceptors, the transphosphorylation of phosphate monoesters ($R-OPO_3H_2$) to yield inorganic phosphate and an alcohol. The product, inorganic phosphate, is also an inhibitor of the enzyme (Fernley & Walker, 1967). The available structures of *Escherichia coli*, human placental and shrimp AP [referred to as ECAP, PLAP and SAP with PDB codes 1alk (Kim & Wyckoff, 1991), 1ew2 (Le Du *et al.*, 2001) and 1k7h (de Backer *et al.*, 2002), respectively] show that the core and the catalytic metal triad have been conserved during evolution. The metal-binding triad is usually occupied by two zinc ions and one magnesium ion (Anderson *et al.*, 1975; Bosron *et al.*, 1977) in binding sites that are commonly referred to as M1, M2 (the zinc-containing sites; Zn1 and Zn2) and M3 (for the Zn/Mg-containing site).

The accepted catalytic mechanism involves a double in-line displacement with the participation of all three metal ions (Kim & Wyckoff, 1991; Holtz & Kantrowitz, 1999; Stec *et al.*, 2000). Zn1 coordinates the leaving group of the substrate for

the first nucleophilic attack and activates an alcohol for the second nucleophilic attack (Gettins & Coleman, 1984; Gettins *et al.*, 1985; Holtz & Kantrowitz, 1999; Holtz *et al.*, 1999). Zn2 coordinates the active-site serine for the first nucleophilic attack and coordinates the substrate. The octahedrally coordinated magnesium ion in M3 coordinates a hydroxide ion that accepts a proton from an adjacent serine before the first nucleophilic attack. Substitution of magnesium with zinc alters the local geometry of the M3 site, so that the optimal configuration for catalysis is lost (Stec *et al.*, 2000). The 3-Zn form of the enzyme has low residual activity but can be activated by magnesium, which replaces zinc in the third site (Cathala & Brunel, 1975; Janeway *et al.*, 1993; Chen *et al.*, 2000; Hung & Chang, 2001). Although the reaction mechanism is mainly based on structural and biochemical data from the *E. coli* enzyme, it is assumed to be generally valid, since structural features and active-site architectures are conserved. However, there must be subtle differences as the mammalian and cold-active APs are more efficient than their prokaryotic homologues (Murphy & Kantrowitz, 1994).

1.1. Metal content and activity

An important difference between the active sites of PLAP, SAP and ECAP resides in position 153, where PLAP and SAP contain histidines (PLAP His153, SAP His149) whilst ECAP has an aspartic acid (ECAP Asp153). Residue 153 has been shown to play an important role in metal binding and thus activity. In mutation studies on ECAP that were designed to mimic mammalian homologues, aspartic acid 153 was mutated to a histidine. The D153H enzyme bound magnesium more weakly than the wild-type (wt) enzyme and needed the addition of magnesium to restore activity (Janeway *et al.*, 1993). The crystal structure showed that the M3 site was occupied by zinc, with the histidine directly coordinated to the zinc ion (Murphy *et al.*, 1995), while the aspartic acid in the wt structure interacts indirectly with the magnesium ion *via* a water molecule (Murphy *et al.*, 1993). The lower magnesium affinity may be explained by the absence of a salt bridge between Asp153 and Lys328, which in the wt enzyme restricts the conformation of Asp153 such that it coordinates a water molecule, which in turn ligates the magnesium ion (Fig. 1). The D153H mutation disrupts this salt link, thus probably destabilizing magnesium coordination.

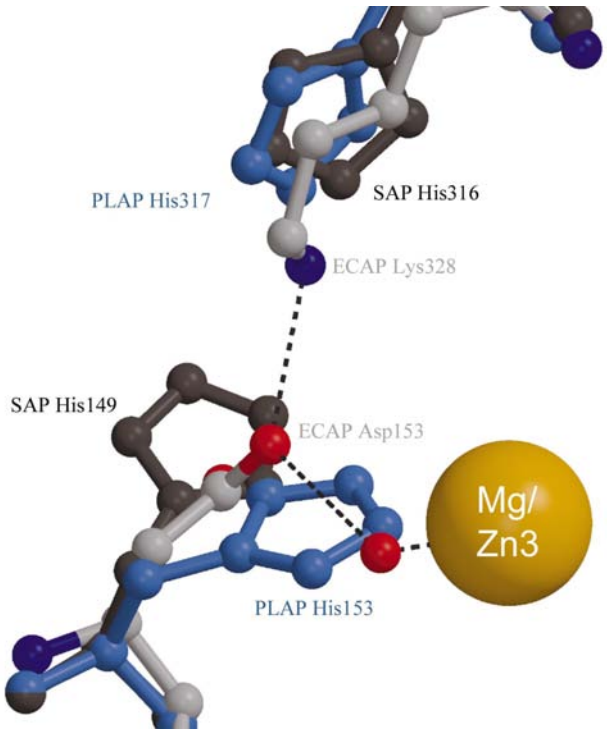

Figure 1
Conformations of residues ECAP Asp153 and Lys328 (coloured by atom) and corresponding residues PLAP His153, PLAP His317 (blue) and SAP His149, SAP His316 (black). The salt bridge between ECAP Asp153 and Lys328 is indicated by a dotted line. Figs. 1, 2 and 3 were prepared with *MOLSCRIPT* (Kraulis, 1991) and *RASTER3D* (Merritt & Bacon, 1997).

There is some controversy concerning the third metal-binding site. It seems that although the presence of zinc reduces activity, mammalian and cold-active enzymes have evolved improved zinc-binding properties in the M3 site. Both PLAP and SAP contain a histidine near the M3 binding site, optimizing it to accommodate zinc. The SAP crystal structure is fully occupied by zinc, with SAP His149 coordinated to the zinc ion at M3 (de Backer *et al.*, 2002). Interestingly, PLAP contains a magnesium ion in M3 (Le Du *et al.*, 2001) and PLAP His153 is not coordinated to the magnesium ion. Why would the M3 site of PLAP, which supposedly has a higher affinity for zinc, still accommodate magnesium? PLAP has been reported to bind magnesium slowly and with low affinity, with zinc acting as a time-dependent inhibitor with a higher binding affinity (Hung & Chang, 2001). Zinc has been suggested to induce a slow conformational change, locking the enzyme in a conformation that has high affinity for zinc but is unfavourable for catalysis. The M3 site may regulate enzyme activity by balancing the lower physiological concentrations of zinc compared with magnesium against the differences in metal-binding affinity (Hung & Chang, 2001).

1.2. Ligand binding

The crystal structures of covalent and non-covalent phosphoenzyme complexes (Kim & Wyckoff, 1991; Murphy *et al.*, 1997; Holtz *et al.*, 1999) show that phosphate inhibits ECAP with one phosphate O atom bound to Zn1, one bound to Zn2 and two to Arg166. This arginine has been shown to be involved in initial binding of the substrate and in the release of inorganic phosphate; mutation of this arginine reduces substrate binding and decreases phosphate inhibition in the absence of phosphate acceptors (Butler-Ransohoff *et al.*, 1988; Chaidaroglou *et al.*, 1988).

1.3. Shrimp alkaline phosphatase

Like many cold-active enzymes, SAP has a high catalytic efficiency and is heat-labile. The high catalytic efficiency of SAP has partly been attributed to optimized surface potentials (de Backer *et al.*, 2002), but details of the active site may provide further explanations for the improved efficiency.

Table 1
Data collection.

Crystallization conditions are described in the text. Values in parentheses are for the highest resolution shell. Sample ID 'PNPP' refers to the soaking experiment with *p*-nitrophenyl phosphate (PNPP) until yellow product was visible. The 'dialyzed sample' refers to the metal-exchange experiment, for which the sample was dialyzed against a $MgCl_2$-containing glycine buffer at pH 10.4.

Sample ID	PNPP	Dialyzed sample
Resolution (Å)	40–2.2 (2.23–2.15)	30–2.0 (2.07–2.00)
Beamline	ID14-2	ID14-4
Wavelength (Å)	0.933	1.2825
R_{merge} (%)	5.4 (15.3)	4.4 (16.4)
Completeness (%)	98.0 (80.6)	98.2 (97.7)
$\langle I\rangle/\sigma(I)$	24.5 (4.2)	26.7 (4.4)
Redundancy	4.5 (3.3)	3.2 (3.2)
Unit-cell parameters (Å)		
$a = b$	170.68	171.01
c	83.93	84.10
Ligand	Phosphate	Sulfate
Metal present in M3	Zn	Mg
R (%)	18.60	21.53
R_{free} (%)	21.82	23.81

The active site of SAP (PDB code 1k7h) has three significant differences from ECAP and PLAP. Firstly, the SAP structure is fully occupied by zinc, as confirmed by anomalous data collected around the absorption edge of zinc, while PLAP and ECAP contain magnesium in site M3. Secondly, SAP His149 is directly coordinated to Zn3, analogously to the ECAP D153H mutant, while the corresponding histidine in PLAP does not coordinate Mg3 (Fig. 1). Thirdly, the arginine that stabilizes inhibitors in ECAP and PLAP (Arg166) has a different conformation in SAP (Arg162). The SAP structure contains no inhibitor and SAP Arg162 has a conformation that could not interact with the ligand. In this study, a crystallization experiment with substrate *p*-nitrophenyl phosphate (PNPP) and a metal-exchange experiment are described. These resulted in conformational changes of Arg162 and His153, respectively.

2. Materials and methods

Shrimp alkaline phosphatase was kindly provided by Biotec Pharmacon (Tromsø, Norway) as an ammonium sulfate precipitate. The enzyme originates from shrimps in the Barents Sea and was purified as described previously (Olsen *et al.*, 1991). The precipitated enzyme was recovered in a 100 m*M* Tris–maleic acid pH 5.6, 1 m*M* $MgCl_2$ and 0.1 m*M* $ZnCl_2$ buffer and was concentrated to 10–15 mg ml^{-1} before crystallization using the hanging-drop vapour-diffusion method. The mother liquor contained 42%(*w*/*v*) saturated ammonium sulfate, 100 m*M* Tris–maleic acid pH 5.6, 1 m*M* $MgCl_2$, 0.1 m*M* $ZnCl_2$ and 5% glycerol. SAP crystallizes in space group $P4_32_12$, with two monomers per asymmetric unit. Before data collection, crystals were washed with a cryoprotectant containing 20–25% glycerol, but without the metals. Crystals were then flash-frozen in the nitrogen stream on the beamline.

Data collection, assisted by *STRATEGY* (Ravelli *et al.*, 1997), was performed on beamline ID14 at the European Synchrotron Radiation Facility in Grenoble. Data for the metal-exchange experiment were collected at the white line of zinc. Data were indexed, processed and scaled with *DENZO* and *SCALEPACK* (Otwinowski & Minor, 1997) or *XDS* (Kabsch, 1993), followed by *TRUNCATE* (French & Wilson, 1978), *CAD*, *SCALEIT* (Howell & Smith, 1992) and *UNIQUEIFY* (Table 1). 5% of the reflections were flagged as R_{free} for cross-validation (Brünger, 1993). Refinement started with rigid-body refinement, followed by restrained refinement of the protein using *REFMAC* (Murshudov *et al.*, 1997). Metal ions were gradually introduced. Omit maps were then calculated, excluding metal ions and active-site residues. Ligands were modelled when $F_o - F_c$ density of at least 3σ had a reasonable size and shape. Manual adjustments were performed with *QUANTA*2000 (Accelrys Inc., 2001). $2F_o - F_c$ electron-density maps were calculated by *FFT* (Immirzi, 1966) using the coefficients FWT and PHWT from *REFMAC* and $F_o - F_c$ electron-density maps were calculated with the coefficients DELFWT and PHDELWT.

2.1. Substrate- and inhibitor-soaking experiments

Hydrolysis of the non-physiological compound *p*-nitrophenyl phosphate (PNPP) has become a general tool for AP activity tests since the reaction product, *p*-nitrophenolate, is yellow and can be followed in colorimetric assays (Kawade, 1964). SAP crystals grown as described above turned bright yellow upon addition of PNPP, thus showing that the enzyme was active in the crystal form. Data sets were collected from

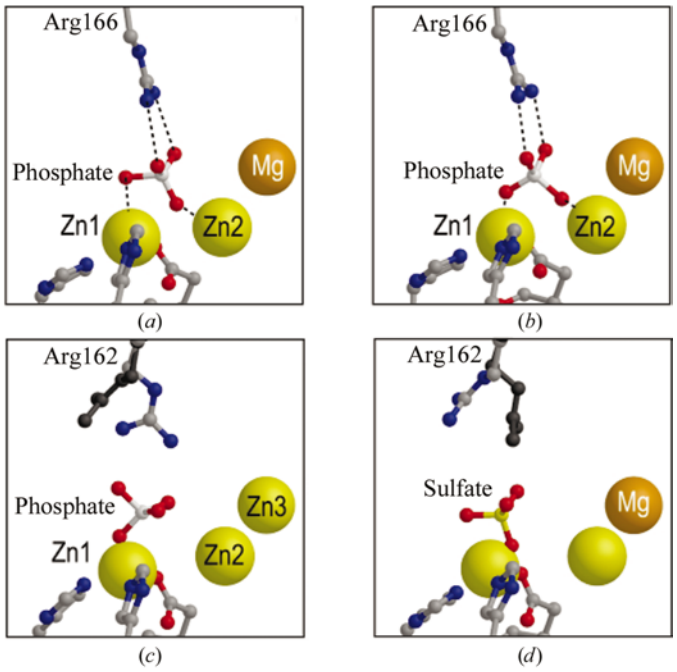

Figure 2
Ligand binding and conformations of the active-site arginine shown for (*a*) the PLAP structure (PDB code 1ew2), (*b*) the ECAP structure (PDB code 1alk) and for SAP structures from (*c*) the PNPP experiment (with phosphate bound) and (*d*) the dialyzed sample (with sulfate bound).

crystals that had been soaked with PNPP for various time intervals and then flash-frozen.

2.2. Enzyme activation and metal exchange

Although SAP is active in the crystal form, its activity is low. This is likely to be because of the presence of zinc in the M3 site (de Backer *et al.*, 2002), despite the tenfold excess of magnesium in the standard crystallization buffer. In an attempt to exchange zinc with magnesium, a two-day dialysis against 0.1 *M* glycine buffer pH 10.4 containing 100 m*M* $MgCl_2$ at 277 K was performed. Crystals were then grown as described above but in the presence of 100 m*M* $MgCl_2$ and no zinc.

3. Results

3.1. Substrate-soaking experiment

The experiments presented in this paper have resulted in refined structures with bound ligands. In each case the ligand was monodentately bound to Zn1, but the orientation varied between the structures. The PNPP substrate-soaking experiment resulted in a structure in which the product phosphate, a known inhibitor, was bound in the active site (Fig. 2*c*). The remainder of the substrate could not be observed at lower σ levels in $2F_o - F_c$ (at 1σ) or $F_o - F_c$ (at 3σ) maps (Fig. 3). The phosphate was monodentately bound to Zn1 with two O atoms hydrogen bonded to the guanidinium group of Arg162. This conformation was analogous to that observed in ECAP and PLAP (Figs. 2*a*, 2*b*, 4*a* and 4*b*), but different from that observed in the MAD structure 1k7h, which does not contain a ligand (Fig. 4*c*).

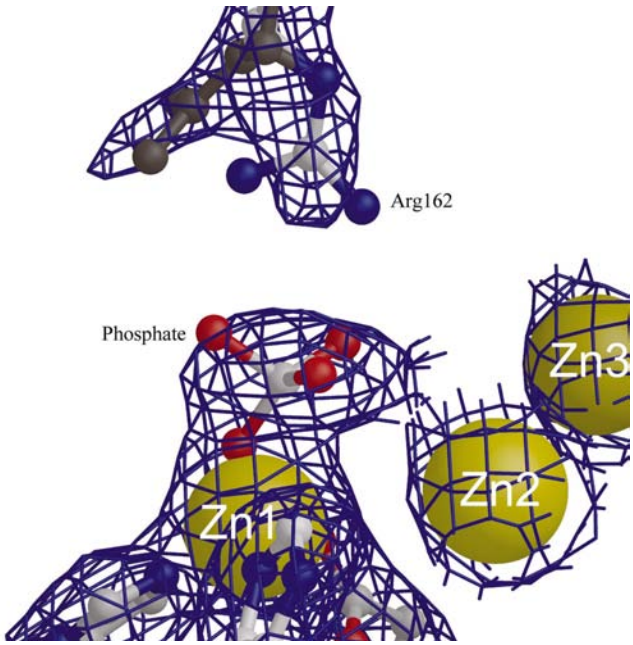

Figure 3
Active-site arginine Arg162 of the substrate (PNPP) soaking experiment shown in two conformations, with Arg162 coloured in its major conformation and in grey in its minor conformation. The $2F_o - F_c$ electron-density map contoured at 1σ. This figure and Fig. 5 were prepared with *BOBSCRIPT* (Esnouf, 1997) and *RASTER3D* (Merritt & Bacon, 1997).

3.2. Metal exchange

The dialysis experiment (§2.2) was expected to result in the replacement of zinc by magnesium at M3. Experiments in which the sample had been dialyzed against a magnesium-containing alkaline glycine buffer showed the presence of magnesium in M3. Anomalous data (collected at the white line of zinc) only indicated the presence of zinc in sites M1 and M2, but significant positive $F_o - F_c$ difference density at M3 indicated that magnesium had replaced zinc. Moreover, His149 was mainly found in the non-coordinated conformation, which also indicates the presence of magnesium (Fig. 5).

This experiment also resulted in a ligand-containing structure. Electron density adjacent to Zn1 suggested a small tetrahedral molecule. Several ions could potentially bind to this site, but the most logical choices were sulfate from the crystallization buffer and the natural inhibitor phosphate. Although these molecules are hardly distinguishable in X-ray diffraction experiments a sulfate molecule was chosen, since a high concentration of ammonium sulfate was present in the crystallization buffer. The modelled sulfate ion was monodentately bound to Zn1 (Fig. 2*d*) with a different orientation to the phosphate group in the PNPP experiment.

4. Discussion

4.1. Ligand binding

Significant and tetrahedral density was observed in the expected phosphate-binding region, but no indications of the presence of the *p*-nitrophenyl group of PNPP were found. This may be explained by the accessible configuration of the active site: an open solvent-exposed cleft that only contains a specific docking site for the phosphate group in substrate molecules. This configuration allows a large degree of mobility for the organic moiety (the '*R* group') of substrates, which makes them difficult to observe in X-ray diffraction experiments. Another very likely explanation is that SAP had hydrolyzed the available substrate molecules before data collection. Taking both considerations into account, a phosphate molecule was modelled.

The orientations of the bound ligands in SAP were different from those observed in PLAP or ECAP. In PLAP, a single phosphate O atom bridges between Zn1 and Zn2 (Fig. 2*a*), whereas in ECAP the phosphate group bridges Zn1 and Zn2, with separate O atoms coordinating each metal ion (Fig. 2*b*). In most other ECAP structures with ligands bound to Zn1, the inhibitors retain this orientation. From this limited set of experiments it is clear that APs do not bind inhibitors in a universal fashion.

4.2. Conformation of the active-site arginine

The active-site arginine is involved in substrate binding and phosphate release (Butler-Ransohoff *et al.*, 1988; Chaidar-

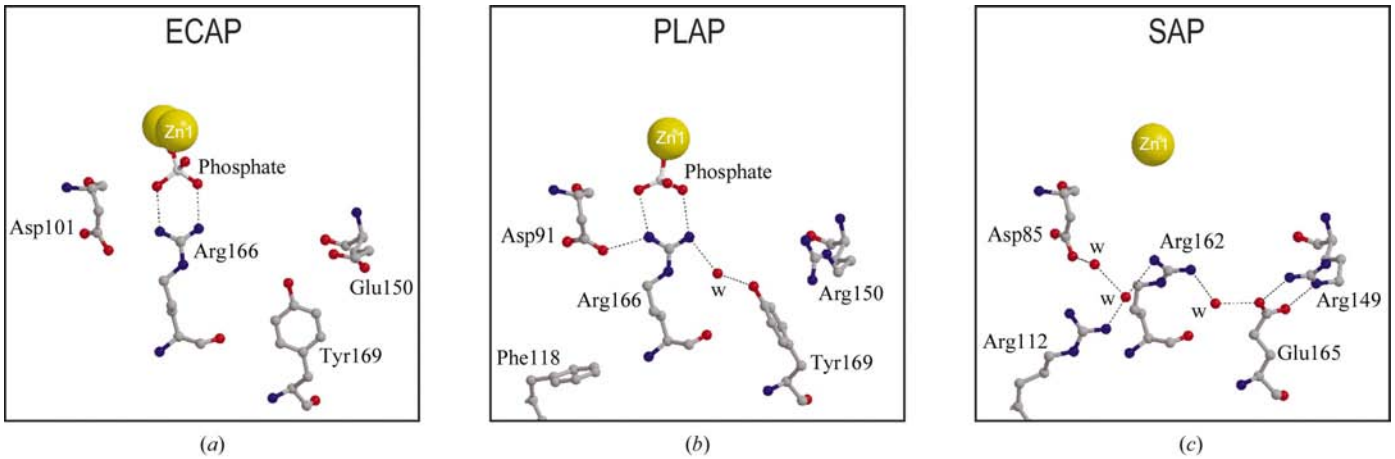

Figure 4
Interactions of the active-site arginine with ligands and neighbouring residues: (*a*) Arg166 in ECAP, (*b*) Arg166 in PLAP and (*c*) Arg162 in SAP (PDB code 1k7h), showing the extensive hydrogen-bonding network that holds SAP Arg162 in a non-coordinated conformation.

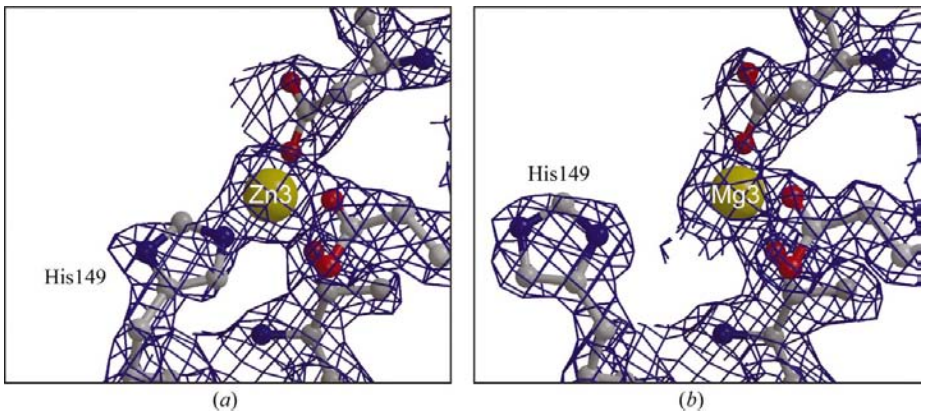

Figure 5
The two conformations of His149 in metal-binding site M3: (*a*) the PNPP structure with His149 in the coordinating conformation and (*b*) the activated structure with the histidine in the non-coordinating position, similar to PLAP His153. The $2F_o - F_c$ maps are contoured at a level of 1.5σ.

oglou *et al.*, 1988). In the structures of ECAP, PLAP and SAP–PNPP the guanidinium group of this arginine directly interacts with two O atoms from the inhibitor (referred to as the 'docked conformation'; Figs. 2*a*, 2*b*, 4*a* and 4*b*), while the MAD and 'dialyzed' SAP structures show Arg162 in a 'non-docked' conformation (Fig. 2*d*).

The active-site arginine has different interactions with neighbouring residues when comparing PLAP, ECAP and SAP (Fig. 4). In all available ECAP structures (with the exception of the D153H/K328H double mutant) Arg166 has identical conformations: it is bound to the inhibitor and may interact with nearby residues Asp101 NH1 and Asp153 OD1. In PLAP the arginine is involved in a hydrogen-bonding network with Arg166 NH1 hydrogen bonded to phosphate and a water molecule that in turn interacts with the hydroxyl group of Tyr169 and another water molecule. Arg166 NH2 interacts with the phosphate group and Asp91 OD1. The arginine conformation in SAP (1k7h) and the dialyzed SAP sample is also controlled by a hydrogen-bonding network, but it interacts indirectly with other residues *via* water molecules. Arg162 NH2 is hydrogen bonded to a water molecule that interacts with Glu165 OE2. This glutamate (corresponding to PLAP Tyr169) is tightly positioned by hydrogen bonds to Arg150 and to Thr148. Arg162 NH1 interacts with a water molecule that in turn interacts with Arg112. This hydrogen bond could not exist in PLAP or ECAP, since PLAP has a phenylalanine at this position (Phe118) and the loop carrying this residue is absent in ECAP. Structural comparison between SAP structures containing Arg162 in the docked position and those containing Arg162 in the non-docked position did not reveal any additional conformational changes of other active-site residues.

It seems that in the absence of inhibitors the non-docked conformation of Arg162 is favourable. The ordered water molecules that provide stabilizing interactions may also allow the arginine to change conformation to interact with bound ligands. It is conceivable that the presence of a ligand is a prerequisite for Arg162 to adopt the docked conformation, although it is not clear which additional conditions apply. It is not likely that the immediate chemical environment of Arg162 changes much when the pH increases from 5.6 (of the crystallization buffer) to physiological pH (pH 7–8), since the amino acids that participate in the hydrogen-bonding network are arginines, aspartic acids and glutamates whose protonation states do not change within this pH range.

The fact that SAP Arg162 does not always interact with a bound ligand may affect the catalytic efficiency and thus the cold-active characteristics of the shrimp enzyme. Based on our structural observations, one may speculate that the substrate/inhibitor is less strongly bound compared with the homologous enzymes. This would facilitate the release of product, which in turn enhances catalytic efficiency. In conjunction with an optimized surface-potential distribution (de Backer *et al.*,

2002), this effect may contribute to the high catalytic efficiency of SAP.

4.3. Metal exchange

The dialysis experiments prove that zinc ions in sites M1 and M2 are strongly bound. Anomalous data showed the presence of zinc in M1 and M2 and that these ions resisted extensive dialysis against high magnesium concentrations. Any zinc present must have been bound in the organism and remained there during purification. The fact that no significant anomalous peaks were observed at M3, while significant $F_o - F_c$ density was present, strongly suggested the presence of magnesium. Moreover, His149 did not coordinate the metal ion in M3 and superimposes with the corresponding histidine in PLAP, which has magnesium bound. These indications strongly suggest the presence of magnesium in M3. In other words, the M3 site seems to have a much higher affinity for zinc than for magnesium, although zinc at M3 can be exchanged for magnesium by extensive dialysis.

In analogy to PLAP (Hung & Chang, 2001), it seems that magnesium binds slowly and with low affinity to SAP, but it is somewhat surprising that it takes quite an effort to accomplish the metal exchange. The dialysis experiment used 100 m*M* $MgCl_2$ and certainly did not resemble physiological conditions, which fall in the low millimolar range. Other experiments using lower concentrations of $MgCl_2$ were not conclusive with regard to the metal content (data not shown). In any case, for X-ray diffraction experiments to observe the magnesium at M3, most SAP molecules in the crystal should exchange zinc with magnesium at this site. This explains why the prolonged dialysis was necessary.

It may well be that the pH plays a crucial role in magnesium binding, since the crystallization buffer had an acidic pH, while the enzyme has an alkaline pH optimum. Magnesium binding in ECAP has been found to decline strongly with decreasing pH (Bosron *et al.*, 1977). If SAP was to have a comparable pH-dependence, the magnesium content at acidic pH (*i.e.* at the pH of the crystallization buffer) would be low. Unfortunately, crystallization trials with various alkaline crystallization buffers failed (even though PLAP and ECAP have been crystallized at alkaline pH) and crystals (obtained at acidic pH) that were soaked in alkaline buffers fragmented after prolonged soaking times. The fragmentation is most likely to indicate rearrangements in the enzyme, which may well be caused by the binding of magnesium.

5. Concluding remarks

Results from our experiments suggest that there is no universal way in which inhibitors bind to alkaline phosphatases. Ligands bound to Zn1 in SAP have different orientations than the molecules bound in ECAP and PLAP. Active-site Arg162 can interact directly with the bound ligand, but it remains unclear which experimental conditions induce a conformational change from a 'non-docked' to a 'docked' conformation, although the presence of a ligand seems to be a prerequisite for this conformational change. The non-docked conformation of Arg162, which is stabilized by a local hydrogen-bonding network, seems favourable and may even enhance catalytic efficiency. Ultimately, insight into inhibitor binding is likely to emerge from site-directed mutagenetic studies, but this lies in the future.

Zinc ions at site M1 and M2 are more strongly bound than at site M3; they are resistant to extensive dialysis against high magnesium concentrations. At the M3 site, zinc ions can be replaced by magnesium ions, resulting in in a reorientation of His149.

References

Accelrys Inc. (2001). *QUANTA*2000. Accelrys Inc., San Diego, CA, USA.

Anderson, R. A., Bosron, W. F., Kennedy, F. S. & Vallee, B. L. (1975). *Proc. Natl Acad. Sci. USA*, **72**, 2989–2993.

Backer, M. de, McSweeney, S., Rasmussen, H. B., Riize, B. W., Lindley, P. & Hough, E. (2002). *J. Mol. Biol.* **318**, 1265–1274.

Bosron, W. F., Anderson, R. A., Falk, M. C., Kennedy, F. S. & Vallee, B. L. (1977). *Biochemistry*, **16**, 610–614.

Brünger, A. T. (1993). *Acta Cryst.* D**49**, 24–36.

Butler-Ransohoff, J. E., Kendall, D. A. & Kaiser, E. T. (1988). *Proc. Natl Acad. Sci. USA*, **85**, 4276–4278.

Cathala, G. & Brunel, C. (1975). *J. Biol. Chem.* **250**, 6046–6053.

Chaidaroglou, A., Brezinski, D. J., Middleton, S. A. & Kantrowitz, E. R. (1988). *Biochemistry*, **27**, 8338–8343.

Chen, Q. X., Zheng, W. Z., Lin, J. Y., Shi, Y., Xie, W. Z. & Zhou, H. M. (2000). *Int. J. Biochem. Cell Biol.* **32**, 879–85.

Collaborative Computational Project, Number 4 (1994). *Acta Cryst.* D**50**, 760–763.

Esnouf, R. M. (1997). *J. Mol. Graph.* **15**, 132–134.

Fernley, H. N. & Walker, P. G. (1967). *Biochem. J.* **104**, 1011–1018.

French, G. S. & Wilson, K. S. (1978). *Acta Cryst.* A**34**, 517–525.

Gettins, P. & Coleman, J. E. (1984). *J. Biol. Chem.* **259**, 4991–4997.

Gettins, P., Metzler, M. & Coleman, J. E. (1985). *J. Biol. Chem.* **260**, 2875–2883.

Holtz, K. M. & Kantrowitz, E. R. (1999). *FEBS Lett.* **462**, 7–11.

Holtz, K. M., Stec, B. & Kantrowitz, E. R. (1999). *J. Biol. Chem.* **274**, 8351–8354.

Howell, P. L. & Smith, G. D. (1992). *J. Appl. Cryst.* **25**, 81–86.

Hung, H. C. & Chang, G. G. (2001). *Protein Sci.* **10**, 34–45.

Immirzi, A. (1966). *Crystallographic Computing Techniques*, edited by F. R. Ahmed, p. 399. Copenhagen: Munksgaard.

Janeway, C. M., Xu, X., Murphy, J. E., Chaidaroglou, A. & Kantrowitz, E. R. (1993). *Biochemistry*, **32**, 1601–1609.

Kabsch, W. (1993). *J. Appl. Cryst.* **26**, 795–800.

Kawade, M. (1964). *Mie Med. J.* **14**, 41–46.

Kim, E. E. & Wyckoff, H. W. (1991). *J. Mol. Biol.* **218**, 449–464.

Kraulis, P. J. (1991). *J. Appl. Cryst.* **24**, 946–950.

Le Du, M. H., Stigbrand, T., Taussig, M. J., Menez, A. & Stura, E. A. (2001). *J. Biol. Chem.* **276**, 9158–9165.

Merritt, E. A. & Bacon, D. J. (1997). *Methods Enzymol.* **277**, 505–524.

Murphy, J. E. & Kantrowitz, E. K. (1994). *Mol. Microbiol.* **12**, 351–357.

Murphy, J. E., Stec, B., Ma, L. & Kantrowitz, E. R. (1997). *Nature Struct. Biol.* **4**, 618–622.

Murphy, J. E., Tibbitts, T. T. & Kantrowitz, E. R. (1995). *J. Mol. Biol.* **253**, 604–617.

Murphy, J. E., Xu, X. & Kantrowitz, E. R. (1993). *J. Biol. Chem.* **268**, 21497–21500.

Murshudov, G. N., Vagin, A. A. & Dodson, E. J. (1997). *Acta Cryst.* D**53**, 240–255.
Olsen, R., Overbo, K. & Myrnes, B. (1991). *Comput. Biochem. Physiol. B*, **99**, 755–761.
Otwinowski, Z. & Minor, W. (1997). *Methods Enzymol* **276**, 307–326.
Ravelli, R. B., Sweet, R. M., Skinner, J. M., Duisenberg, A. J. M. & Kroon, J. (1997). *J. Appl. Cryst.* **30**, 551–554.
Stec, B., Holtz, K. M. & Kantrowitz, E. R. (2000). *J. Mol. Biol.* **299**, 1303–1311.
Vincent, J. B., Crowser, M. W. & Averill, B. A. (1992). *Trends Biol. Sci.* **17**, 105–110.